Extremophiles
DOI 10.1007/s00792-008-0150-1

ORIGINAL PAPER

A novel metabolic network leads to enhanced citrate biogenesis in *Pseudomonas fluorescens* exposed to aluminum toxicity

Ryan J. Mailloux · Joseph Lemire · Sergey Kalyuzhnyi · Vasu Appanna

Received: 23 November 2007 / Accepted: 6 February 2008

Abstract Aluminum (Al), an environmental toxin, is known to have a negative impact on various biological systems. However, some microbes have devised intricate mechanisms to combat the toxic influence of this trivalent metal. In this study, *Pseudomonas fluorescens* grown in malate invoked a unique metabolic shift to promote the synthesis of citrate, a metabolite involved in the sequestration of Al. Electrophoretic and spectrophotometric assays revealed several malate-metabolizing enzymes including malate dehydrogenase (MDH) and malic enzyme (ME) displayed increases in activity and expression in the Al-treated cells. Whereas pyruvate dehydrogenase (PDH) also showed increased activity and expression in the Al-stressed cultures, phosphoenolpyruvate carboxykinase (PEPCK) displayed a marked diminution in the Al-treated cells. The upregulation of citrate synthase (CS) coupled with the diminished activities of aconitase (ACN) and NAD-isocitrate dehydrogenase (NAD-ICDH) appeared to be instrumental in the accumulation of citrate. HPLC experiments revealed high levels of citrate in the Al-stressed cultures. Thus, an Al-enriched environment provoked a metabolic shift in *P. fluorescens* dedicated to the conversion of malate to citrate.

Communicated by G. Antranikian.

R. J. Mailloux · J. Lemire · V. Appanna (✉)
Department of Chemistry and Biochemistry,
Laurentian University, Sudbury, ON, Canada P3E 2C6
e-mail: vappanna@laurentian.ca

S. Kalyuzhnyi
Department of Chemical Enzymology, Moscow State University, 119992 Moscow, Russia

Keywords Aluminum · Malate · Citrate · Metabolic adaptation · Malic enzyme · Citrate synthase

Abbreviations

ME	Malic enzyme
MDH	Malate dehydrogenase
PEPCK	Phosphoenol pyruvate carboxykinase
ACN	Aconitase
PDH	Pyruvate dehydrogenase
CS	Citrate synthase
NAD-ICDH	NAD-dependent isocitrate dehydrogenase
Al	Aluminum

Introduction

Despite its ubiquity, Al displays no role in biological systems. Indeed, this trivalent metal has been conveniently excluded from biological functions due to its unfavorable chemical attributes. Although Al is considered innocuous due to its insolubility at neutral pH, acid rain, industrial activity, and pollution have made this inert metal more bioavailable to bacteria, plants, and humans (Becaria et al. 2002; Nayak 2002). Al is notorious for its deleterious effects on biological systems. Ca-mediated processes, membrane bilayers, and Mg-catalyzed reactions have been shown to be some of the primary targets of Al (Pina and Cervantes 1996; MacDiarmid and Gardner 1998; Yoshino et al. 1999; Kawano et al. 2003). In addition, Al exhibits pro-oxidant activities and is capable of displacing Fe from enzymatic sites (Oshiro et al. 1998; Crichton et al. 2002). Indeed, the ability of Al to alter membrane fluidity, disrupt Fe homeostasis, and promote oxidative stress can be a recipe that is disastrous to most life forms.

Since Al is capable of disrupting Fe homeostasis and promoting reactive oxygen species (ROS) generation, enzymes involved in aerobic respiration are potent targets of the toxic influence of this metal. We have previously reported that the exposure of both eukaryotes and prokaryotes to Al results in disturbed aerobic metabolism and an energy deficit within the cell (Mailloux et al. 2006a, b, 2007a, b). Aerobic energy metabolism is inherently dependent on the presence of Fe to produce the necessary ATP molecules to support cellular processes. Tricarboxylic acid (TCA) cycle enzymes, such as aconitase (ACN) and succinate dehydrogenase, and the respiratory complexes require Fe-S clusters and heme groups for their enzymatic activities. Indeed, a variety of organisms rely on aerobic metabolism for survival. However, in the presence of Al, aerobic energy is severely compromised leading to a dearth of available energy and, subsequently, the demise of the cell.

In order to survive an Al-enriched environment, the soil microbe *P. fluorescens* tailors the TCA cycle to detoxify this toxic metal. For instance, Al-exposed *P. fluorescens* grown in citrate-containing cultures produce α-ketoglutarate and oxalate in order to sequester ROS and detoxify Al. While α-ketoglutarate accumulates as a consequence of the Al-mediated deactivation of α-ketoglutarate dehydrogenase, oxalate is generated by the upregulation of isocitrate lyase (Appanna et al. 2003; Mailloux et al. 2007a, b). *P. fluorescens* exposed to Al is also known to increase the production of NADPH in order to maintain the antioxidant defense system (Singh et al. 2005a, b). Indeed, malic enzyme (ME), glucose-6-phosphate dehydrogenase, and NADP-ICDH, the three NADPH-producing enzymes, display increased activity in Al-treated cells. ME and NADP-ICDH are closely associated with the TCA cycle generating NADPH as well as pyruvate and α-ketoglutarate for antioxidant defense. Furthermore, the *P. fluorescens* exposed to Al is characterized by the diminished activity of NADH-producing enzymes within the TCA cycle in an effort to control the evolution of ROS from the respiratory complexes. Thus, in the presence of Al, *P. fluorescens* is known to alter a variety of metabolic pathways in order to detoxify Al and quell oxidative stress.

In the present study, in an effort to further delineate the significance of metabolic networks in cellular survival, we have evaluated the metabolic changes associated with the detoxification of Al in *P. fluorescens* grown in malate. In the presence of an Al-enriched environment, this microbe invokes a metabolic alteration designed to transform malate into citrate, a detoxifier of Al. ME, Malate dehydrogenase (MDH), and Pyruvate dehydrogenase (PDH) play crucial roles in this process in order to generate NADPH and produce oxaloacetate and acetyl CoA, two ingredients central for the biogenesis of citrate. Furthermore, the loss of ACN and NAD-dependent isocitrate dehydrogenase (NAD-ICDH) activity promotes the accumulation of citrate. The significance of this metabolic shift in molecular detoxification and evolution is discussed.

Material and methods

Microbial growth conditions, biomass determination, and cellular fractionation

Pseudomonas fluorescens (ATCC 13525) was from the American Type Culture Collection and was maintained and grown in a mineral medium consisting of Na_2HPO_4 (0.06 g), KH_2PO_4 (0.03 g), NH_4Cl (0.8 g), $MgSO_4.7H_2O$ (0.2 g), and 20 mM malate (2.7 g) per litre of deionized water. Trace elements were present in concentrations as described previously (Anderson et al. 1992). In the Al-stressed medium, malic acid was complexed to $AlCl_3{\cdot}6H_2O$ (10 mM) in a molar ratio of 2:1. The pH was adjusted to 6.8 with 1N NaOH. The media was then dispensed into 200 ml amounts and autoclaved. The media were inoculated with 1 ml of stationary-phase cells grown in an Al-free medium in an aerated gyratory water bath shaker, model 76 (New Brunswick Scientific) at 26°C at 140 rpm. Biomass was monitored by measuring solubilized proteins. Bovine serum albumin (BSA) was used as the standard (Sapan et al. 1999).

The bacterial cells were harvested at similar growth phases (28 h for control and 32 h for Al-stressed) and then resuspended in a cell storage buffer (CSB) consisting of 50 mM Tris-HCl, 5 mM $MgCl_2$, 1 mM PMSF and 1mM DTT (pH 7.3). Following the sonication of the cells, soluble cell-free extract (CFE) and membrane CFE were obtained by centrifugation (Singh et al. 2007). These CFE fractions were kept at 4°C for up to 5 days and various enzymatic activities were monitored.

Enzymatic assays

The activity of several enzymes was assayed using an Ultraspec Pro 3100 spectrophotometer. The activities of ME, MDH, and PDH were monitored at 450 nm with the aid of 2,4-dinitrophenyl hydrazine (DNPH) (Romanov et al. 1999). ME activity was assayed by incubating a 0.2-mg protein equivalent to soluble fraction in reaction buffer (25 mM Tris-HCl 5 mM $MgCl_2$, pH 7.3), 0.2 mM NADP, and 2 mM malate. The production of pyruvate was monitored at 450 nm with 2,4-dinitrophenyl hydrazine (DNPH). The activity of MDH was ascertained in a similar fashion except 0.2 mg of membrane protein was exposed to malate and NAD. PDH activity was also measured by incubating 0.1 mg of protein equivalent to the membrane

fraction in reaction buffer, 0.2 mM pyruvate in the presence of 0.2 mM NAD, and 0.1 mM CoA. Pyruvate and oxaloacetate were used as standards for these assays. ACN activity was detected by following the formation of *cis*-aconitate (Middaugh et al. 2005). The liberation of CoA by citrate synthase (CS) was assessed at 412 nm using 5, 5′-dithio-bis-2-nitrobenzoic acid (DTNB). A reaction mixture containing reaction buffer, 2 mM oxaloacetate, 2 mM acetyl CoA, and a 0.2 mg protein equivalent to soluble protein was used to monitor CS (Farrell et al. 1984). Reactions were performed for 300 s. Reactions devoid of protein or substrate served as negative controls.

Polyacrylamide gel electrophoresis, activity staining, and immunoblot analysis

Blue Native polyacrylamide gel electrophoresis (BN PAGE) was performed as described previously (Beriault et al. 2005; Singh et al. 2005a, b; Mailloux et al. 2006a, b). To ensure optimal protein separation, 4–16% linear gradient gels were cast with the Bio-Rad MiniProtean^{TM} 2 system using 1-mm spacers. Soluble or membrane protein weighing 60 μg was loaded into the wells and the gels were electrophoresed under native conditions. The blue cathode buffer (50 mM Tricine, 15 mM Bis-Tris, 0.02% (w/v) Coomassie G-250 (pH 7) at 4°C) was changed to a colorless cathode buffer (50 mM Tricine, 15 mM Bis-Tris, (pH 7) at 4°C) when the running front was half-way through the gel. The in-gel visualization of enzyme activity was ascertained by coupling the formation of NAD(P)H to 0.3 mg/mL of phenazine methosulfate (PMS) and 0.5 mg/mL of iodonitrotetrazolium (INT). ME activity was visualized with malate and NADP as substrates. For MDH, NAD was utilized. The in-gel activity of PDH was assessed with pyruvate, NAD, and CoA. Phosphoenol pyruvate carboxykinase (PEPCK) and ACN were visualized by coupling their in-gel activities to exogenous enzymes. ACN was detected with the aid of NADP-ICDH while PEPCK was visualized with MDH (Middaugh et al. 2005; Singh et al. 2005a, b). NADH oxidase was detected by incubating the gel slab in reaction buffer containing 0.5 mM NADH, 5 mM KCN, INT, and 5 mM rotenone. The activity of NADH kinase was visualized using an enzyme-coupled assay as described in Singh et al. (2007). Reactions were stopped using destaining solution (40% methanol, 10% glacial acetic acid) once the activity bands reached their desired intensity. The resulting bands were documented and used for 2D BN-PAGE SDS-PAGE analysis. Activity bands were quantified using SCION imaging software.

SDS-PAGE and 2D SDS-PAGE gels were performed in accordance with the modified method described in Laemmli (1970), Mailloux et al. (2006a, b). For SDS-PAGE and immunoblot, 30 μg of protein was solubilized in 62.5 mM Tris-HCl (pH 6.8), 2% SDS, and 2% β-mercaptoethanol at 100°C for 5 min. Following solubilization, the protein samples were then loaded into a 10% isocratic gel and electrophoresed using a discontinuous buffer system. The proteins were then electroblotted to a Hybond^{TM}—Polyvinylidene difluoride membrane for immunoblotting as described in Singh et al. (2007). Primary antibodies directed against PDH were used to ascertain the levels of this protein. The PDH antibody was a generous gift from Dr. Lindsay (University of Glasgow). The secondary antibody consisted of a horseradish peroxidase conjugated to an antirabbit antibody (Sigma). Following several washings the membrane was dried and probed for 5 min at room temperature with Chemiglow reagent (Alpha Innotech). The immunoblot was documented using a ChemiDoc XRS system (Biorad Imaging Systems). For 2D BN-PAGE SDS-PAGE analysis, activity bands from native gels were precision cut from the gel and incubated in denaturing buffer (1% β-mercaptoethanol, 5% SDS) for 30 min, and then loaded vertically into the SDS gel. Electrophoresis was carried out as described above. Proteins were detected by Coomassie staining.

Time profile experiments and analysis of citrate levels

Cells were harvested as described previously. At different time intervals, cells were isolated and disrupted by sonication to yield membrane and soluble fractions. The fractions were treated as described above. Activity staining was performed accordingly in an effort to monitor the temporal dependence of the activities of ME and MDH in control and Al-stressed cultures.

The presence of citrate in the media was assessed using HPLC. Media were collected following a 28 and 32-h exposure to control and Al-stressed conditions, respectively. The samples were injected into an Alliance HPLC equipped with a C_{18} reverse-phase column (Synergi Hydro-RP; 4 μm; 250 x 4.6 mm, Phenomenex) operating at a flow rate of 0.7 mL/min at ambient temperature. The proper separation of citrate from the other metabolites was achieved using a mobile phase consisting of 20 mM K_2HPO_4 (pH 2.9). The presence of citrate in the media was monitored at 210 nm. Citrate was identified by injecting known standards individually and by spiking various samples with citrate. Enzymatic assays involving ACN were also employed to confirm the presence of this tricarboxylic acid.

Statistical analysis

Data were expressed as mean ± SD. Statistical correlations of data were checked for significance using the

student t test. Experiments were performed twice and in triplicate.

Results and discussion

Aluminum promotes citrate accumulation and alterations in malate-metabolizing enzymes

In the presence of 10 mM Al, *P. fluorescens* grown in a malate-containing medium experienced a significant decline in growth rate (Fig. 1, I). Although, the stationary growth phase in the Al-exposed cultures was attained 4 h after the control cultures, the biomass was relatively the same. Thus, it appeared that the Al-challenged cells had adapted to the presence of this toxic metal. In order to probe the nature of this adaptation, the spent fluid from the control and Al-stressed cultures were analyzed by HPLC. These experiments were carried out on cultures from similar growth phases (28 h for control and 32 h for Al-stressed cultures, respectively). In contrast to control cultures, an abundance of citrate was observed in the Al-stressed cultures (Fig. 1, II). The nature of this metabolic response was probed by assessing the specific activity of several enzymes involved in the metabolism of malate and citrate. ME and MDH, two enzymes involved in the oxidation of malate to pyruvate and oxaloacetate, displayed a 1.5 and a twofold increase in activity in *P. fluorescens* exposed to Al (Table 1). Similarly, the activities of PDH and CS, two enzymes involved in the production of acetyl CoA and citrate, were found to be 7.5 and twofold higher in the Al-stressed cells. In contrast, ACN activity was diminished by twofold in the Al-treated cells. Thus, the presence of Al evokes a metabolic response which promotes the conversion of malate to citrate.

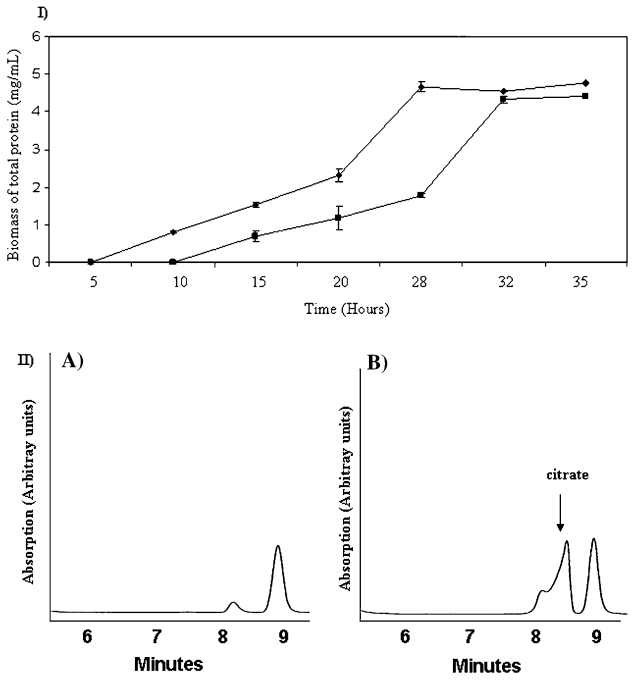

Fig. 1 Citrate accumulates in cell cultures exposed to Al. **I** Growth of *P. fluorescens* in control (*filled diamond*) and Al-stressed (*filled square*) cultures over a 35 h period. Bacteria were isolated at various time intervals and then solubilized to determine total protein content. **II** The detection of citrate in the media from (*A*) control and (*B*) Al-stressed cultures. Following a 28 and 32-h exposure to control or Al-stressed conditions, the media was isolated and treated accordingly for HPLC analysis. Samples were injected into a C_{18} reverse phase column operating at flow rate of 0.7 mL/min. 20 mM KH_2PO_4 was used as the mobile phase to afford the proper separation of the metabolites. Citrate was identified by injecting known standards

In order to probe the nature of these metabolic alterations further, we analyzed the activity and expression of ME and MDH. BN-PAGE analysis revealed a sharp increase in the activity of ME in cells exposed to Al for 32 h (Fig. 2a, I). 2D BN-PAGE SDS-PAGE and coomassie staining revealed a significant amount of protein associated with the activity bands from the Al-stressed cultures (Fig. 2a, II). A marked increase in ME activity was recorded at 25 h incubation in Al, an observation that was evident up to 40 h (Fig. 2a, III). Similar to ME, the in-gel activity of MDH was increased in the Al-exposed cells. Indeed, a sharp band corresponding to MDH was recorded in membrane fraction isolated from *P. fluorescens* cultured in Al for 32 h (Fig. 2b, I). The increase in MDH activity was associated with increased protein content. Indeed, 2D BN-PAGE SDS-PAGE analysis of the activity bands revealed a marked increase in the MDH protein levels (Fig. 2b, II). Time profile analysis of MDH activity provided further insight into the impact of Al on

Table 1 The specific activities of selected enzymes in *P. fluorescens* exposed to control or Al-stressed conditions for 28 and 32 h, respectively

Enzyme	Control cultures	Al-stressed cultures
Malic enzyme[a]	1.448 (±0.024)	2.009 (±0.070)*
Malate dehydrogenase[a]	0.311 (±0.021)	0.806 (±0.014)*
Pyruvate dehydrogenase[a]	0.080 (±0.073)	0.665 (±0.053)*
Aconitase[b]	0.0142 (± 0.003)	0.0065 (±0.004)*
Citrate synthase[c]	0.026 (±0.011)	0.048 (±0.003)*

Cells were isolated at similar growth phases

Units: mmol of products formed min-1 mg protein-1 $n = 3$, mean ± S.D., $P \leq 0.05$

*Denotes a significant difference in comparison to the control

All reactions were performed for 300 s

[a] Activity measured using DNPH

[b] Activity measured by detecting the double bond of cis-aconitate

[c] Activity measured using DTNB

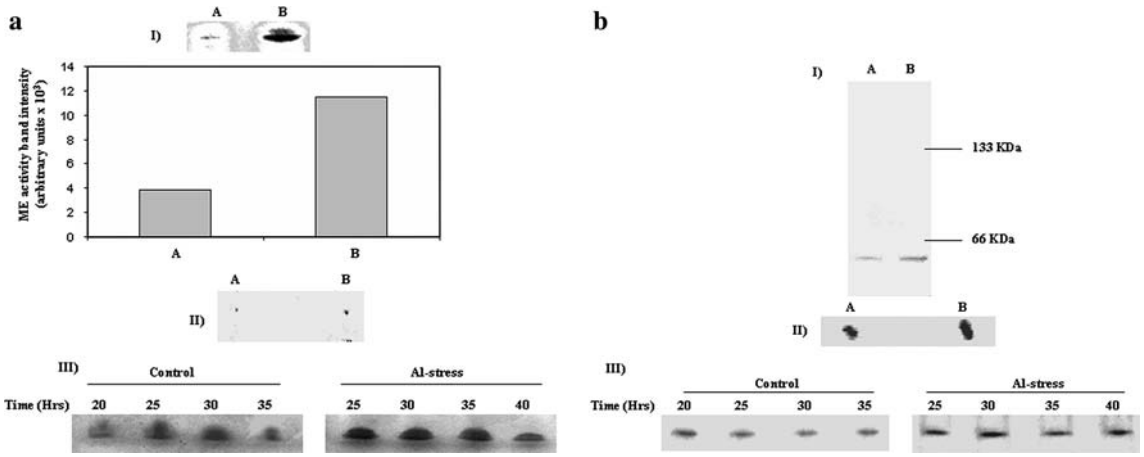

Fig. 2 **a** Activity and expression of ME in *P. fluorescens* exposed to (*A*) control or (*B*) Al-stressed cultures. *I* In-gel detection of ME activity. Activity bands were quantified using SCION imaging software. *II* 2D BN-PAGE SDS-PAGE analysis of ME levels in control and Al-stressed cells. The activity bands from *I* were excised, treated with 1% SDS solution, and then loaded into the wells of the SDS-PAGE gel. Proteins were detected by staining the gel slab with Coomassie R-250. NOTE: Cells from the control and Al-stressed cultures were isolated at the same growth phase. Control cells were grown for 28 h and Al-stressed cells were grown for 32 h unless otherwise indicated. *III* Time-dependent profile of ME activity in cells isolated from control and Al-stressed cultures. **b** Activity and expression of MDH in *P. fluorescens* exposed to (*A*) control or (*B*) Al-stressed cultures. *I* In-gel detection of MDH activity. *II* 2D BN-PAGE SDS-PAGE analysis of MDH levels in control and Al-stressed cells. The activity bands from *I* were excised, treated with 1% SDS solution, and then loaded into the wells of the SDS-PAGE gel. Proteins were detected by staining the gel slab with Coomassie R-250. NOTE: Cells from the control and Al-stressed cultures were isolated at the same growth phase. Control cells were grown for 28 h and Al-stressed cells were grown for 32 h unless otherwise indicated. *III* Time-dependent profile of MDH activity in cells isolated from control and Al-stressed cultures

P. fluorescens. A sharp increase in MDH activity was observed after 25 h of exposure to Al (Fig. 2b, III).

The Al-treated cells displayed a marked increase in PDH activity, a key enzyme in citrate biogenesis (Fig. 3a, I). Immunblot assays using antibodies directed against the E_2-subunit of PDH revealed a sharp increase in the E_2-subunit of PDH in the Al-stressed cells in contrast to the control (Fig. 3a, II). The E_2-subunit of PDH was previously reported to be approximately 45 KDa (Komuniecki et al. 1992). Thus, the presence of Al increased the activity and expression of PDH. The increase in the activity and expression of MDH prompted us to discern the effect of Al on PEPCK. In the Al-stressed cells, PEPCK displayed a decrease in activity in contrast to the control cells (Fig. 3a, III). The molecular mass of the monomeric PEPCK enzyme has been predicted to be between 65–80 KDa (Mukhopadhyay et al. 2001; Aich et al. 2003). Indeed, 2D BN-PAGE SDS-PAGE analysis of the activity bands pointed to a reduced amount of PEPCK enzyme in the Al-stressed cells (Fig. 3a, IV). In the Al-stressed cells, a sharp increase in CS activity was observed in contrast to the Al-stressed cells (Table 1). The augmented activity of CS coincided with an increased amount of protein. SDS-PAGE analysis of the soluble proteins revealed that Al toxicity promoted the expression of this enzyme in comparison to control fractions (Fig. 3b, I). Thus, the increased activity and expression of CS would enhance the condensation of oxaloacetate and acetyl CoA to produce citrate. The accumulation of citrate in the Al-treated cultures was also due to the diminution of ACN and NAD-ICDH activity. These two enzymes were affected severely by the presence of Al (Fig. 3b, II, III).

Although the upregulation of MDH is crucial to the metabolic adaptation to Al, the NADH generated by this reaction cannot be oxidized by the respiratory complexes. Indeed, we have shown previously that Al severely hampers the activity and expression of the respiratory complexes (Mailloux et al. 2007a, b). NADH oxidase would play a key role in regenerating NAD for MDH and PDH. In addition, NADH kinase may play a part in producing the NADPH, a key factor required for antioxidant defense. Thus, we hypothesized that these two enzymes contribute to the metabolic adaptation of *P. fluorescens* to Al toxicity. In contrast to the control cells, NADH oxidase displayed a sharp increase in activity in the Al-exposed cells (Fig. 3c, I). However, 2D BN-PAGE SDS-PAGE analysis of the activity bands revealed no significant change in the expression of NADH oxidase (Fig. 3c, II). This is surprising since the expression of NADH oxidase increases in Al-exposed *P. fluorescens* grown in citrate (data not shown). In the Al-stressed condition, the activity of NADH kinase was also augmented (Fig. 3c, III). 2D BN-PAGE SDS-PAGE analysis revealed high amounts of protein associated with the activity bands from the

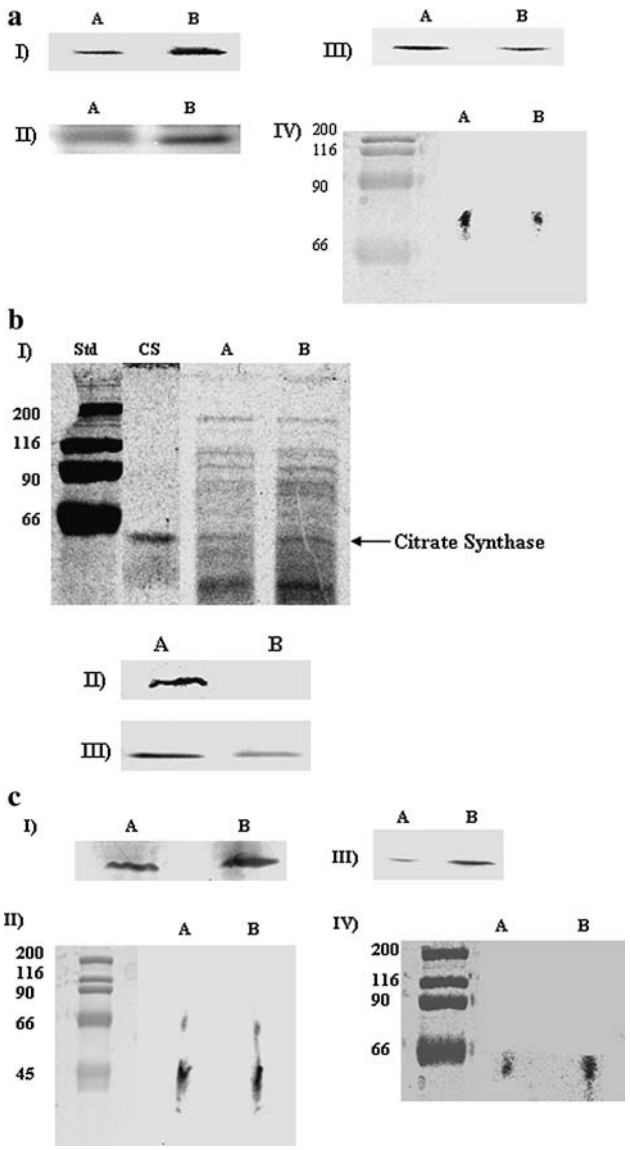

◀ **Fig. 3 a** Activity and expression of PDH and PEPCK in *P. fluorescens* exposed to (*A*) control or (*B*) Al-stressed cultures. *I* In-gel detection of PDH activity. *II* The immunoblot detection of PDH expression. *III* In-gel detection of PEPCK activity. *IV* 2D BN-PAGE SDS-PAGE analysis of PEPCK levels in control and Al-stressed cells. The activity bands from *III* were excised, treated with 1% SDS solution, and then loaded into the wells of the SDS-PAGE gel. Proteins were detected by staining the gel slab with Coomassie R-250. NOTE: Cells from the control and Al-stressed cultures were isolated at the same growth phase. Control cells were grown for 28 h and Al-stressed cells were grown for 32 h unless otherwise indicated. **b** The determination of the activity and expression of several enzymes involved in citrate metabolism in *P. fluorescens* exposed to (*A*) control or (*B*) Al-stressed conditions. *I* The expression of citrate synthase in control and Al-stressed cells. The CFE was prepared in Laemmli buffer and the proteins were electrophoresed in an SDS gel. Proteins were detected by Coomassie staining. CS corresponds to 1 μg of citrate synthase standard. *II* The in-gel detection of ACN activity. *III* The in-gel detection of NAD-ICDH activity. NOTE: Cells from the control and Al-stressed cultures were isolated at the same growth phase. Control cells were grown for 28 h and Al-stressed cells were grown for 32 h unless otherwise indicated. **c** The determination of the activity and expression of NADH oxidase and NADH kinase in *P. fluorescens* exposed to (*A*) control or (*B*) Al-stressed conditions. *I* The in-gel detection of NADH oxidase. *II* 2D BN-PAGE SDS-PAGE analysis of NADH oxidase levels in control and Al-stressed cells. The activity bands from *I* were excised, treated with 1% SDS solution, and then loaded into the wells of the SDS-PAGE gel. Proteins were detected by staining the gel slab with Coomassie R-250. *III* The in-gel detection of NADH kinase activity. *IV* 2D BN-PAGE SDS-PAGE analysis of NADH oxdase levels in control and Al-stressed cells. The activity bands from *III* were excised, treated with 1% SDS solution, and then loaded into the wells of the SDS-PAGE gel. Proteins were detected by staining the gel slab with Coomassie R-250. NOTE: Cells from the control and Al-stressed cultures were isolated at the same growth phase. Control cells were grown for 28 h and Al-stressed cells were grown for 32 h unless otherwise indicated

Al-stressed cells (Fig. 3c, IV). Thus, it appears that NADH oxidase and NADH kinase do contribute to the survival of *P. fluorescens* during Al toxicity.

Although metabolic pathways are known as discrete entities, they can be reconfigured to meet the needs of the cell. Situations such as metal toxicity and oxidative stress are known to induce numerous metabolic reconfigurations in order to sustain energy production and the survival of an organism (Imlay 2002; Fedotcheva et al. 2006; Lemire et al. 2007; Marino et al. 2007). For instance, *P. fluorescens* exposed to the superoxide-producing molecule menadione invokes a metabolic shift aimed at limiting NADH production and enhancing NADPH generation (Singh et al. 2007). *P. fluorescens* deliberately modifies the TCA cycle and the glyoxylate shunt in order to detoxify Al and ROS molecules (Appanna et al. 2003; Mailloux et al. 2007a, b). Indeed, alterations in these critical metabolic pathways allow this organism to survive an extreme environment.

Thus, it is not surprising to find that various elements from different metabolic pathways converge together to create a unique module to ensure the survival of the organism. In the present study, Al toxicity evoked a metabolic response aimed at transforming malate into citrate. The alterations in the activity and expression of several key enzymes involved in malate metabolism would enable the cell to detoxify Al and ROS. The upregulation of ME would play a pivotal role in allowing the organism to cope with oxidative stress. This enzyme generates both pyruvate and NADPH, two crucial antioxidant defense molecules (Alvarez et al. 2003; Valderrama et al. 2006). In this instance, ME is upregulated in Al-malate exposed cells in order to produce NADPH and pyruvate. Thus, the type of carbon source may dictate the type of response an organism may initiate. It appears that enzymes from several metabolic pathways coalesced in order to promote survival of this microbe confronted with Al toxicity. Although MDH and PEPCK are involved in the TCA cycle and gluconeogenesis respectively, in this instance they work in

tandem to generate the ingredients critical for the biogenesis of citrate. While MDH showed a sharp increase in activity and expression, PEPCK displayed an opposite trend. This response would ensure that abundant levels of oxaloacetate are available for citrate production.

The presence of Al triggered the accumulation of citrate, a tricarboxylic acid implicated in the detoxification of Al. Indeed, Al resistance in some leguminous plants is achieved by enhanced citrate release from roots (Ligaba et al. 2004). The enhanced production of citrate has been attributed to an increase in CS and a concomitant decrease in ACN (Anoop et al. 2003). However, the importance of PDH in the overproduction of citrate has never been demonstrated. In the present study, the upregulation of PDH and CS and the downregulation of ACN and NAD-ICDH ensure the accumulation of citrate, an Al-detoxifying agent. The role of PDH in this process is paradoxical since this enzyme is quite sensitive to oxidation (Cabiscol et al. 2000). Indeed, PDH contains a lipoic acid residue on its E_2-subunit which is crucial for the production of NADH. However, in the presence of ROS, the thiol on the lipoic acid is oxidized rendering the enzyme inactive. We have shown previously that Al, Ga, and ROS deactivate α-ketoglutarate dehydrogenase by oxidizing the lipoic acid residue in its E_2-subunit (Mailloux et al. 2007a, b). Oxaloacetate and acetyl CoA are well-known feedback inhibitors for the MDH and PDH enzymes (Hansford 1976; Mottram and Coombs 1985). Thus, the CS activity maintains low levels of oxaloacetate and acetyl CoA by forming citrate. The decrease in ACN and NAD-ICDH also contributes to the accumulation of citrate. The ability of Al to disrupt ACN activity is attributed to its ability to perturb the Fe-S (Middaugh et al. 2005). Thus, the loss of ACN activity would promote the accumulation of citrate. Furthermore, the loss of NAD-ICDH activity would also contribute to citrate accumulation. Indeed, this enzyme has been shown to be a rate-limiting enzyme for citrate metabolism in the TCA cycle (Zhao and McAlister-Henn 1996). Thus, Al toxicity in malate-grown cells evokes a unique metabolic shift aimed at the accumulation of citrate, a potent detoxifier of Al.

NADH oxidase and NADH kinase also appeared to play a significant role in the metabolic response of *P. fluorescens* towards Al toxicity. While NADH oxidase catalyzes the conversion of NADH to NAD, NADH kinase phosphorylates NADH to produce NADPH. We have previously shown that the respiratory complexes are severely impeded by Al (Mailloux et al. 2007a, b). Thus, NADH oxidase would play a pivotal role in removing NADH in an effort to maintain MDH and PDH activity. It

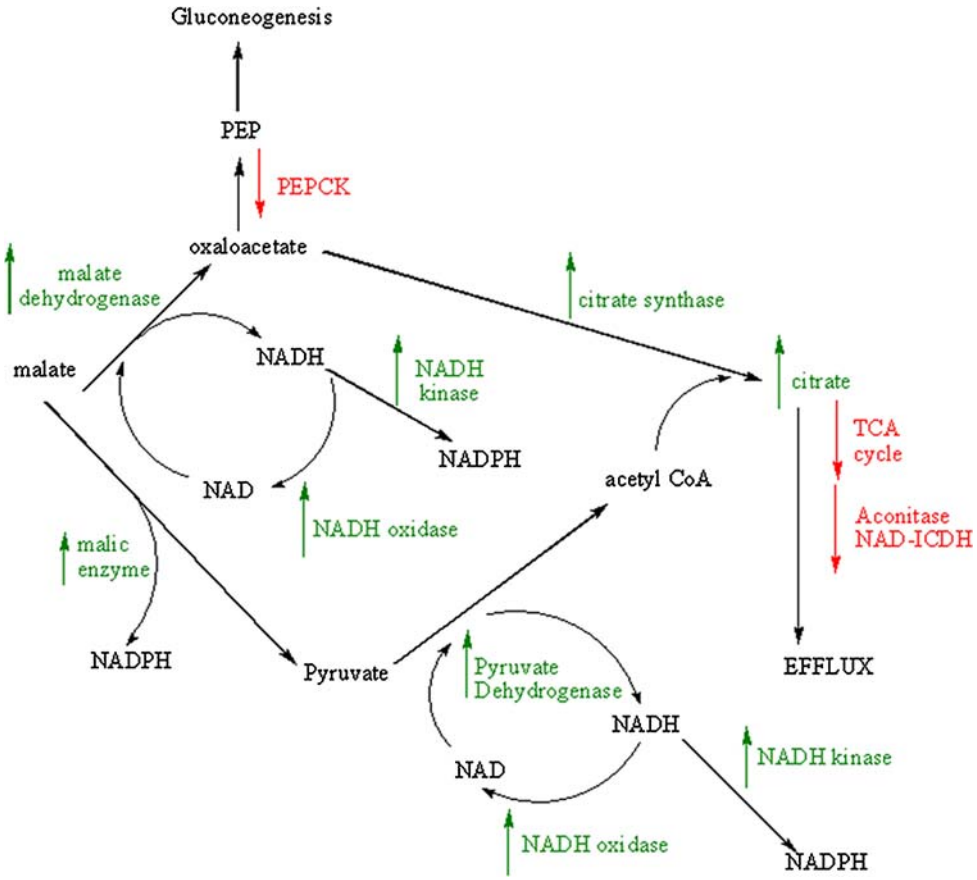

Fig. 4 *P. fluorescens* incorporates different elements from various pathways in order to create a unique metabolic module to combat Al toxicity. *PEPCK* phosphoenolpyruvate carboxykinase, *TCA* tricarboxylic acid, *NAD-ICDH* NAD-dependent isocitrate dehydrogenase, *PEP* phosphoenolpyruvate. *Up arrow* increase, *down arrow* decrease

is tempting to speculate that NADH oxidase works in unison with MDH and PDH in order to maintain a constant supply of oxaloacetate and acetyl CoA. NADH kinase also displayed an increase in activity in the Al-treated cells. The NADH generated by PDH and MDH would serve as a substrate for NADPH production. Thus, NADH oxidase and NADH kinase form a critical partnership to ensure the survival of *P. fluorescens* in an Al-enriched environment.

In conclusion, Al toxicity elicits a metabolic response in *P. fluorescens* aimed at promoting the survival of this organism. This is achieved by incorporating different metabolic enzymes from disparate metabolic pathways. This metabolic reconfiguration results in a unique metabolic module dedicated to the production of citrate, a metabolite known to render Al innocuous. These data clearly illustrate how an organism can deliberately alter discrete metabolic pathways to create new ones in an effort to meet its needs. Indeed, the ability of an organism to change its biochemical profile in response to environmental cues is the cornerstone of survival and evolution. It is not unlikely that the tailoring of metabolism to specific condition may be the precursor of all metabolic pathways. Figure 4 illustrates the metabolic adaptation of *P. fluorescens* exposed to Al chelated to malate. Thus, Al toxicity triggers a series of biochemical changes characterized by the alteration of several key enzymes involved in the TCA cycle, gluconeogenesis, and NADH transformation that work in a symbiotic fashion for the survival of the organism.

Acknowledgments This work was funded by Ontario Center of Excellence and the Northern Ontario Heritage Fund.

References

Aich S, Imabayashi F, Delbaere LT (2003) Expression, purification, and characterization of a bacterial GTP-dependent PEP carboxykinase. Protein Expr Purif 31(2):298–304

Alvarez G, Ramos M, Ruiz F, Satrustegui J, Bogonez E (2003) Pyruvate protection against beta-amyloid-induced neuronal death: role of mitochondrial redox state. J Neurosci Res 73(2):260–269

Anderson S, Appanna VD, Huang J, Viswanatha T (1992) A novel role for calcite in calcium homeostasis. FEBS Lett 308(1):94–96

Anoop VM, Basu U, McCammon MT, McAlister-Henn L, Taylor GJ (2003) Modulation of citrate metabolism alters aluminum tolerance in yeast and transgenic canola overexpressing a mitochondrial citrate synthase. Plant Physiol 132(4):2205–2217

Appanna VD, Hamel RD, Levasseur R (2003) The metabolism of aluminum citrate and biosynthesis of oxalic acid in *Pseudomonas fluorescens*. Curr Microbiol 47(1):32–39

Becaria A, Campbell A, Bondy SC (2002) Aluminum as a toxicant. Toxicol Ind Health 18(7):309–320

Beriault R, Chenier D, Singh R, Middaugh J, Mailloux R, Appanna V (2005) Detection and purification of glucose 6-phosphate dehydrogenase, malic enzyme, and NADP-dependent isocitrate dehydrogenase by blue native polyacrylamide gel electrophoresis. Electrophoresis 26(15):2892–2897

Cabiscol E, Piulats E, Echave P, Herrero E, Ros J (2000) Oxidative stress promotes specific protein damage in *Saccharomyces cerevisiae*. J Biol Chem 275(35):27393–27398

Crichton RR, Wilmet S, Legssyer R, Ward RJ (2002) Molecular and cellular mechanisms of iron homeostasis and toxicity in mammalian cells. J Inorg Biochem 91(1):9–18

Farrell SO, Fiol CJ, Reddy JK, Bieber LL (1984) Properties of purified carnitine acyltransferases of mouse liver peroxisomes. J Biol Chem 259(21):13089–13095

Fedotcheva NI, Sokolov AP, Kondrashova MN (2006) Nonezymatic formation of succinate in mitochondria under oxidative stress. Free Radic Biol Med 41(1):56–64

Hansford RG (1976) Studies on the effects of coenzyme A-SH: acetyl coenzyme A, nicotinamide adenine dinucleotide: reduced nicotinamide adenine dinucleotide, and adenosine diphosphate: adenosine triphosphate ratios on the interconversion of active and inactive pyruvate dehydrogenase in isolated rat heart mitochondria. J Biol Chem 251(18):5483–5489

Imlay JA (2002) How oxygen damages microbes: oxygen tolerance and obligate anaerobiosis. Adv Microb Physiol 46:111–153

Kawano T, Kadono T, Furuichi T, Muto S, Lapeyrie F (2003) Aluminum-induced distortion in calcium signaling involving oxidative bursts and channel regulation in tobacco BY-2 cells. Biochem Biophys Res Commun 308(1):35–42

Komuniecki R, Rhee R, Bhat D, Duran E, Sidawy E, Song H (1992) The pyruvate dehydrogenase complex from the parasitic nematode *Ascaris suum*: novel subunit composition and domain structure of the dihydrolipoyl transacetylase component. Arch Biochem Biophys 296(1):115–121

Laemmli UK (1970) Cleavage of structural proteins during the assembly of the head of bacteriophage T4. Nature 227(5259):680–685

Lemire J, Mailloux R, Appanna VD (2007) Zinc toxicity alters mitochondrial metabolism and leads to decreased ATP production in hepatocytes. J Appl Toxicol (in press)

Ligaba A, Shen H, Shibata K, Yamamoto Y, Tanakamaru S, Matsumoto H (2004) The role of phosphorus in aluminium-induced citrate and malate exudation from rape (*Brassica napus*). Physiol Plant 120(4):575–584

MacDiarmid CW, Gardner RC (1998) Overexpression of the *Saccharomyces cerevisiae* magnesium transport system confers resistance to aluminum ion. J Biol Chem 273(3):1727–1732

Mailloux R, Lemire J, Appanna V (2007a) Aluminum-induced mitochondrial dysfunction leads to lipid accumulation in human hepatocytes: a link to obesity. Cell Physiol Biochem 20(5):627–638

Mailloux RJ, Beriault R, Lemire J, Singh R, Chenier DR, Hamel RD, Appanna VD (2007b) The tricarboxylic acid cycle, an ancient metabolic network with a novel twist. PLoS ONE 2(1):e690

Mailloux RJ, Hamel R, Appanna VD (2006a) Aluminum toxicity elicits a dysfunctional TCA cycle and succinate accumulation in hepatocytes. J Biochem Mol Toxicol 20(4):198–208

Mailloux RJ, Singh R, Appanna VD (2006b) In-gel activity staining of oxidized nicotinamide adenine dinucleotide kinase by blue native polyacrylamide gel electrophoresis. Anal Biochem 359(2):210–215

Marino D, Gonzalez EM, Frendo P, Puppo A, Arrese-Igor C (2007) NADPH recycling systems in oxidative stressed pea nodules: a key role for the NADP+ -dependent isocitrate dehydrogenase. Planta 225(2):413–421

Middaugh J, Hamel R, Jean-Baptiste G, Beriault R, Chenier D, Appanna VD (2005) Aluminum triggers decreased aconitase activity via Fe-S cluster disruption and the overexpression of isocitrate dehydrogenase and isocitrate lyase: a metabolic network mediating cellular survival. J Biol Chem 280(5):3159–3165

Mottram JC, Coombs GH (1985) Purification of particulate malate dehydrogenase and phosphoenolpyruvate carboxykinase from *Leishmania mexicana mexicana*. Biochim Biophys Acta 827(3):310–319

Mukhopadhyay B, Concar EM, Wolfe RS (2001) A GTP-dependent vertebrate-type phosphoenolpyruvate carboxykinase from *Mycobacterium smegmatis*. J Biol Chem 276(19):16137–16145

Nayak P (2002) Aluminum: impacts and disease. Environ Res 89(2):101–115

Oshiro S, Kawahara M, Mika S, Muramoto K, Kobayashi K, Ishige R, Nozawa K, Hori M, Yung C, Kitajima S, Kuroda Y (1998) Aluminum taken up by transferrin-independent iron uptake affects the iron metabolism in rat cortical cells. J Biochem (Tokyo) 123(1):42–46

Pina RG, Cervantes C (1996) Microbial interactions with aluminium. Biometals 9(3):311–316

Romanov V, Merski MT, Hausinger RP (1999) Assays for allantoinase. Anal Biochem 268(1):49–53

Sapan CV, Lundblad RL, Price NC (1999) Colorimetric protein assay techniques. Biotechnol Appl Biochem 29(Pt 2):99–108

Singh R, Beriault R, Middaugh J, Hamel R, Chenier D, Appanna VD, Kalyuzhnyi S (2005a) Aluminum-tolerant *Pseudomonas fluorescens*: ROS toxicity and enhanced NADPH production. Extremophiles 9(5):367–373

Singh R, Chenier D, Beriault R, Mailloux R, Hamel RD, Appanna VD (2005b) Blue native polyacrylamide gel electrophoresis and the monitoring of malate- and oxaloacetate-producing enzymes. J Biochem Biophys Methods 64(3):189–199

Singh R, Mailloux RJ, Puiseux-Dao S, Appanna VD (2007) Oxidative stress evokes a metabolic adaptation that favors increased NADPH synthesis and decreased NADH production in *Pseudomonas fluorescens*. J Bacteriol 189(18):6665–6675

Valderrama R, Corpas FJ, Carreras A, Gomez-Rodriguez MV, Chaki M, Pedrajas JR, Fernandez-Ocana A, Del Rio LA, Barroso JB (2006) The dehydrogenase-mediated recycling of NADPH is a key antioxidant system against salt-induced oxidative stress in olive plants. Plant Cell Environ 29(7):1449–1459

Yoshino M, Ito M, Haneda M, Tsubouchi R, Murakami K (1999) Prooxidant action of aluminum ion–stimulation of iron-mediated lipid peroxidation by aluminum. Biometals 12(3):237–240

Zhao WN, McAlister-Henn L (1996) Assembly and function of a cytosolic form of NADH-specific isocitrate dehydrogenase in yeast. J Biol Chem 271(17):10347–10352